Propulsion and Power Research 2013;2(1):50–55

http://ppr.buaa.edu.cn/

Propulsion and Power Research

www.sciencedirect.com

ORIGINAL ARTICLE

Finite element analysis of propellant of solid rocket motor during ship motion

Kai Qu*, **Xudong Zhang**

Department of Aircraft Engineering, Naval Aeronautical and Astronautical University, Yantai, Shandong 264001, China

Received 8 March 2012; accepted 17 December 2012
Available online 21 March 2013

KEYWORDS

Shipborne missile;
Solid rocket motor;
Propellant;
Finite element analysis;
Mises stress

Abstract In order to simulate the stress and strain of solid rocket motors (SRMs), a finite element analysis model was established. The stress spectra of the SRM elements with respect to time in the case that the vessel cruises under a certain shipping condition were obtained by simulation. According to the analysis of the simulation results, a critical zone was confirmed, and the Mises stress amplitudes of the different critical zones were acquired. The results show that the maximum stress and strain of SRM are less than the maximum tensile strength and elongation, respectively, of the propellant. The cumulative damage of the motor must also be evaluated by random fatigue loading.

1. Introduction

Solid rocket motors (SRMs) have the advantages of a simple structure and convenient manufacturing; therefore, they have been widely applied to navy weapon systems in China. With the development of the national economy, the navy of China is taking on the responsibility of protecting the country's trade course. Because of this, naval vessels will cruise the important sea areas for an extended period of time. For example, the country sends vessels to the Aden gulf every year to protect the merchantmen. In those seas, wind and ocean waves may be extremely treacherous [1,2]. The propellant grain of the SRM could result in cracking and/or dewetting in these storage conditions. These significant problems are induced by the stress and strain in the SRM propellant, which are undetectable by current non-destructive inspection methods. It is important to simulate the stress and strain in the SRM propellant, because it confirms the critical area and assists in evaluating the damage of the motor [3–6].

*Corresponding author: Tel.: +86 535 6635574.
E-mail address: qu_kai_1980@sina.com (Kai Qu).

Peer review under responsibility of National Laboratory for Aeronautics and Astronautics, China.

Production and hosting by Elsevier

2212-540X © 2013 National Laboratory for Aeronautics and Astronautics. Production and hosting by Elsevier B.V. All rights reserved.
http://dx.doi.org/10.1016/j.jppr.2012.12.002

Nomenclature

T	time (unit: s)
E	relaxation modulus (unit: MPa)
K	bulk modulus (unit: MPa)
G	shearing modulus (unit: MPa)
u	displacement (unit: m)

Greek letters

ρ	density (unit: kg/m^3)
μ	Poisson ratio
α	comparative modulus
τ	relaxation time (unit: s)
σ	stress (unit: Pa)

Subscripts

0	instantaneous modulus
e	equilibrium modulus

The SRM was selected as the object in the middle part of some naval vessel. First, a three-dimensional (3D) model was established from the dimensions and structure of the SRM. Next, the stress and strain of the SRM propellant were simulated with respect to the acceleration loading. Finally, the critical area was confirmed by analysing the simulation results.

2. 3D model of SRM

In order to analyse the stress of the SRM, a 3D model of the motor needs to be established. The motor in this study is made up of a case, liner, and propellant, which are shown in Figure 1. The motor was designed to reduce the stress concentration, by enabling the head and the afterbody with artificial debonds.

Because the acceleration loading in each direction is different, the simulation uses the entire 3D model. However, Figure 1 in order to properly depict the inner structure of the motor, 1/5 of the entire 3D model was selected. It is made up of a pentagram propellant, case, liner, and artificial debonds, which are shown in Figure 2.

3. Materials properties

The materials properties of the propellant, liner, and case are listed in Table 1.

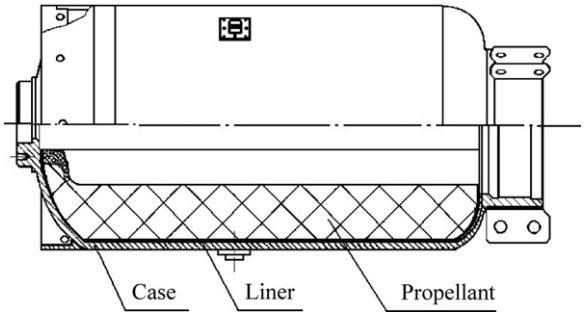

Figure 1 Schematic of an SRM.

The relaxation modulus of the propellant in Table 1 is expressed in Eq. (1) [7].

$$E(t) = 1.799 + 1.43e^{-t/0.04} + 2.05e^{-t/0.4} + 3.05e^{-t/4} + 3.9e^{-t/40} \quad (1)$$

The bulk modulus and shearing modulus can be computed by Eq. (2) and Eq. (3), respectively.

$$K(t) = \frac{E(t)}{3(1-2\mu)} \quad (2)$$

$$G(t) = \frac{E(t)}{2(1+\mu)} \quad (3)$$

According to Eq. (1), Eqs. (2) and (3) can be transformed to Eqs. (4) and (5), respectively.

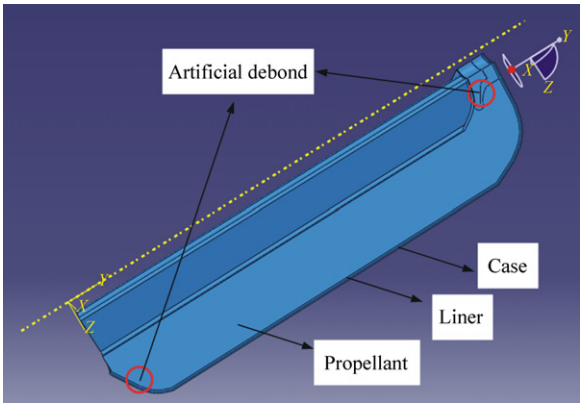

Figure 2 1/5 model of an SRM.

Table 1 Properties of materials.

	P/(kg/m^3)	μ	E/MPa
Propellant	1.7×10^3	0.495	$E(t)$
Liner	1.28×10^3	0.495	12.18
Case	7.85×10^3	0.3	206.9×10^3

$$G(t) = G_e + \sum_{i=1}^{n} G_i \exp\left(-\frac{t}{\tau_i}\right) \tag{4}$$

$$K(t) = K_e + \sum_{i=1}^{n} K_i \exp\left(-\frac{t}{\tau_i}\right) \tag{5}$$

The instantaneous bulk modulus and instantaneous shearing modulus can be acquired by Eqs. (6) and (7), respectively.

$$G_0 = G(t=0) = G_e + \sum_{i=1}^{n} G_i \tag{6}$$

$$K_0 = K(t=0) = K_e + \sum_{i=1}^{n} K_i \tag{7}$$

The comparative bulk modulus and comparative shearing modulus are defined as in Eq. (8).

$$\alpha_i^G = G_i/G_0, \quad \alpha_i^K = K_i/K_0 \tag{8}$$

The material properties can be acquired by the above equations using simulation.

4. Boundary conditions

The SRM is fixed to the launch box by a dowel. The coordinate system is selected according to the motor coordinate system, which is fixed to the SRM. The displacement of the motor outside the boundary is zero, as shown in Eq. (9).

$$u_i = 0 \quad (i = r, z, \theta) \tag{9}$$

When the motor is not ignited, the inside boundary is a free boundary, as shown in Eq. (10).

$$\sigma_r = 0 \tag{10}$$

In order to carry out the finite element analysis, the boundary conditions are selected by a former analysis.

5. Loading conditions

The loading of the SRM while it is at sea correlates with the sea state and shipping conditions. In the simulation, the sea state was 5 and the speed of the ship was 14 knots at 135° abaft the beam. The motor is located in a missile launch box that is distanced 40 m from the vessel head. The angle of missile emission is 15°. According to the theory of ship seakeeping [8], the ship's motion can be simulated. Based on the results of the ship's motion, the acceleration of the motor can be computed in the inertial coordinate system. The acceleration can be transformed to the motor coordinate system by the d'Alembert principle. The acceleration is shown in Figures 3–5.

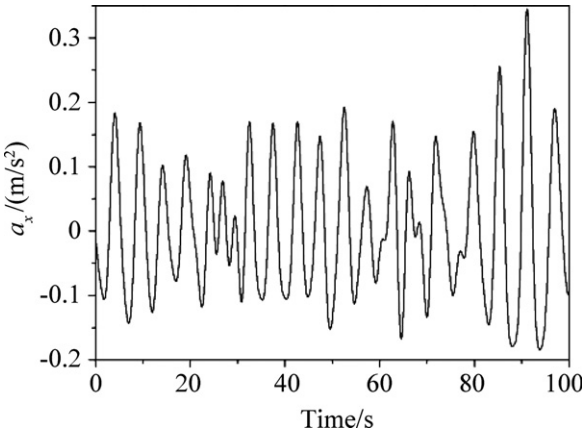

Figure 3 *X*-axis acceleration vs. time of motor.

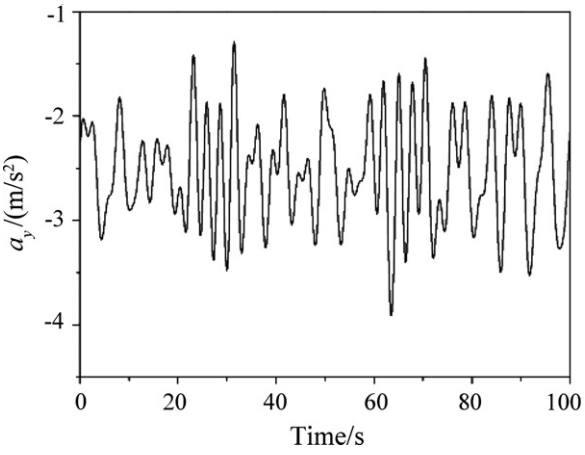

Figure 4 *Y*-axis acceleration vs. time of some motor.

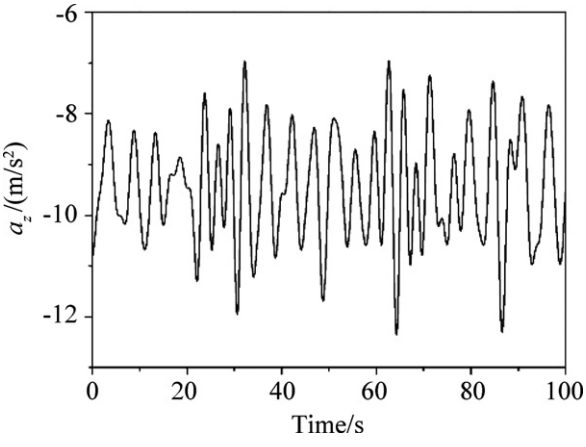

Figure 5 *Z*-axis acceleration vs. time of motor.

6. Computing grid

In order to calculate the stress and strain of the motor by the finite element method, the model needs to include a grid partition, which uses tetrahedral shapes. The grid number is 859,601, as shown in Figure 6.

7. Results

7.1. Stress and strain of motor with respect to time

The simulation used 8 CPUs. The main frequency of each one is 2.33 GHz. The memory is 12 GB and the loading step is 1000. The time step is 0.1 s. The stress and strain of the motor are acquired over 100 s. The stress and strain are shown in Figure 7 and Figure 8, respectively, at 32 s.

According to the results, the maximum Mises stress of the grain at 32 s is 2.101 kPa and the maximum principal strain of the grain at 32 s is 1.305×10^{-3}. The maximum stress and strain areas are located in the upward-facing part of the motor afterbody. The values of the maximum stress and strain are less than the tensile strength and elongation, respectively, of the propellant. Consequently, the propellant of the motor does not get destroyed by instantaneous loading. However, this fatigue from loading can cause cumulative damage. Therefore, the stress and strain should be conserved. Because the computational data is large, conserving all data is impractical. In order to economise stress and strain data storage space, the critical area must be found.

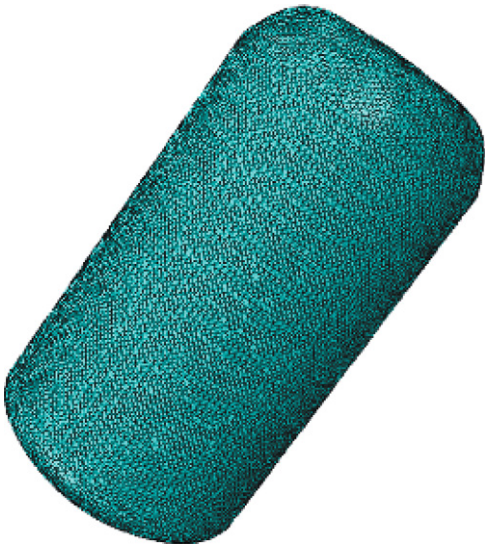

Figure 6 Finite-element grid of a solid rocket motor.

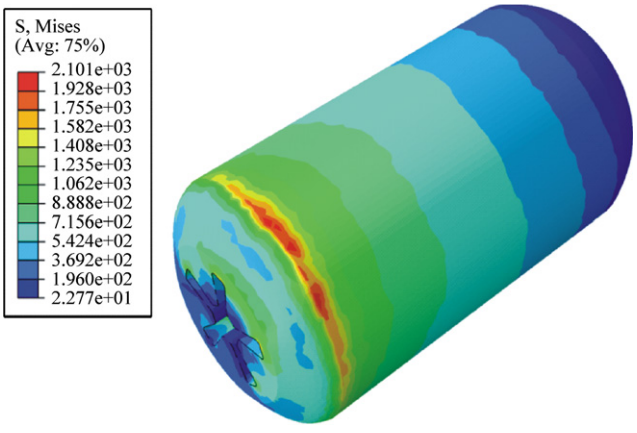

Figure 7 Mises stress of a grain at 32 s.

7.2. Propellant critical area confirmation

In order to find the critical area, three paths and one section are selected. The paths are distinguished by red '▲', red '■', and a blue line, which are shown in Figure 9. These paths are defined path 1, path 2, and path 3. Path 1 and path 2 separately locate the

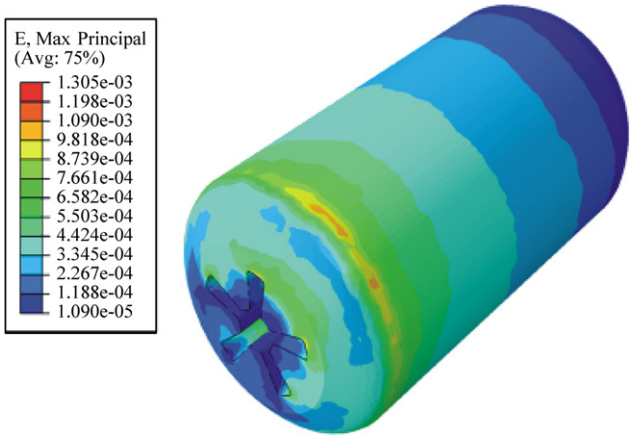

Figure 8 Principal strain of a grain at 32 s.

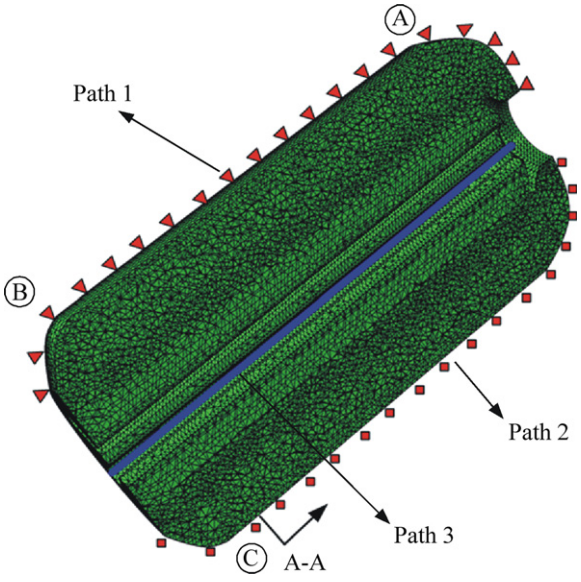

Figure 9 Paths of a grain.

upward-facing surface and downward-facing surface in section yoz of the motor coordinate system. Path 3 lies in the star corner of the grain across the head of the afterbody. Section A-A is near the afterbody, which is where the maximum stress of the inner grain is at 32 s. Path 4, shown in Figure 10, is in the section A-A, which is formed by the red shapes outlining motion along the inner grain.

Firstly, the stress in these paths should be studied at 32 s, because the maximum stress region may appear in the paths. The stress distribution in these paths is shown in Figure 11.

The critical areas are selected as A, B, C, and D, which correspond to the four paths' maximum Mises stresses in Figure 11.

According to the analysis of Figure 11, the maximum Mises stress is not located in the head or the afterbody because the artificial debonds release the stress concentration in those two areas.

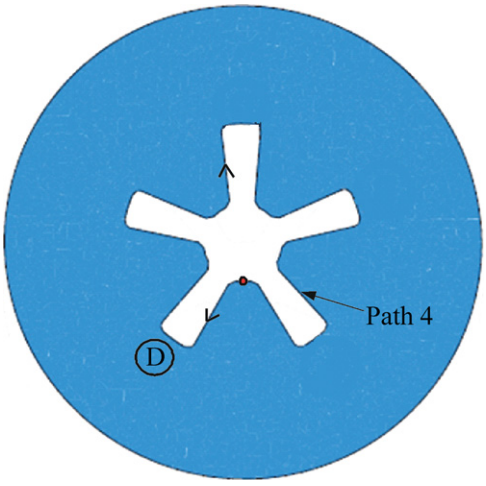

Figure 10 Path of section A-A.

7.3. Mises stress spectrum of critical area in motor

According to the simulation results, the Mises stress spectrum of critical areas in the motor can be acquired. The plot of the Mises stresses of the dangerous areas (A, B, C, and D) versus time is shown in Figure 12. The maximum Mises stress amplitude is in critical area B, and the minimum Mises stress amplitude is in critical area D.

8. Conclusions

From simulations of the stress and strain of SRM by finite element analysis, two conclusions can be drawn:

(1) The maximum stress and strain of SRMs are less than the maximum tensile strength and elongation, respectively.

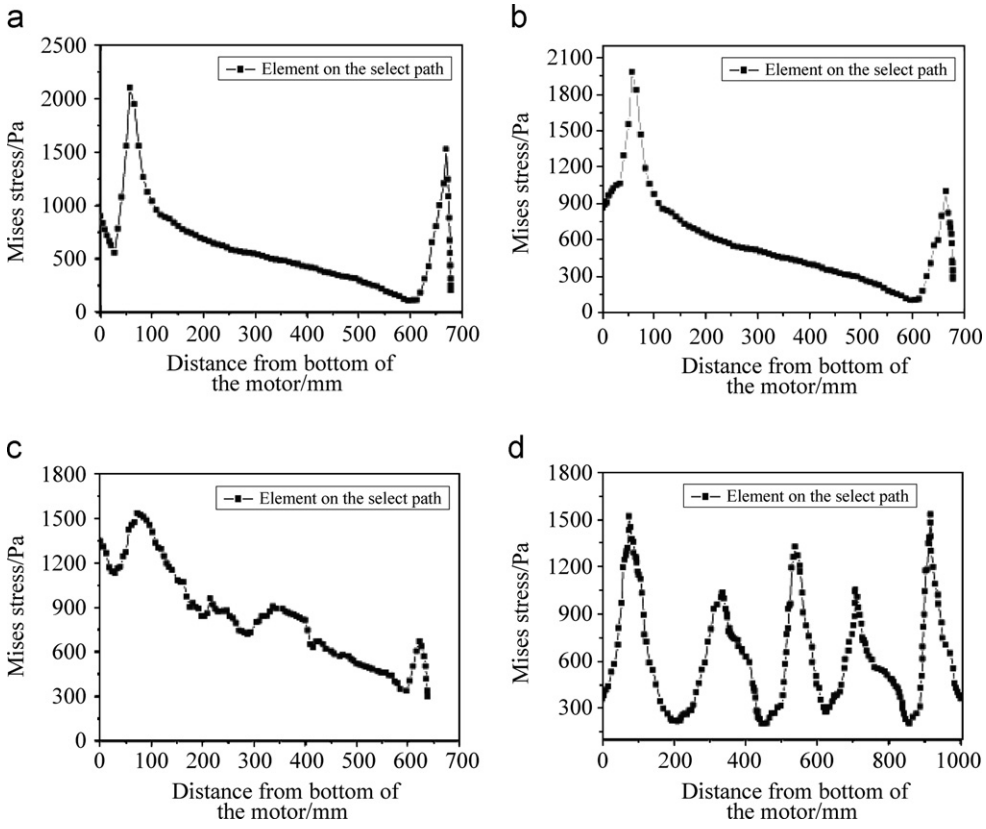

Figure 11 Mises stress for four paths in a grain. (a) Mises stress of path 1, (b) Mises stress of path 2, (c) Mises stress of path 3 and (d) Mises stress of path 4.

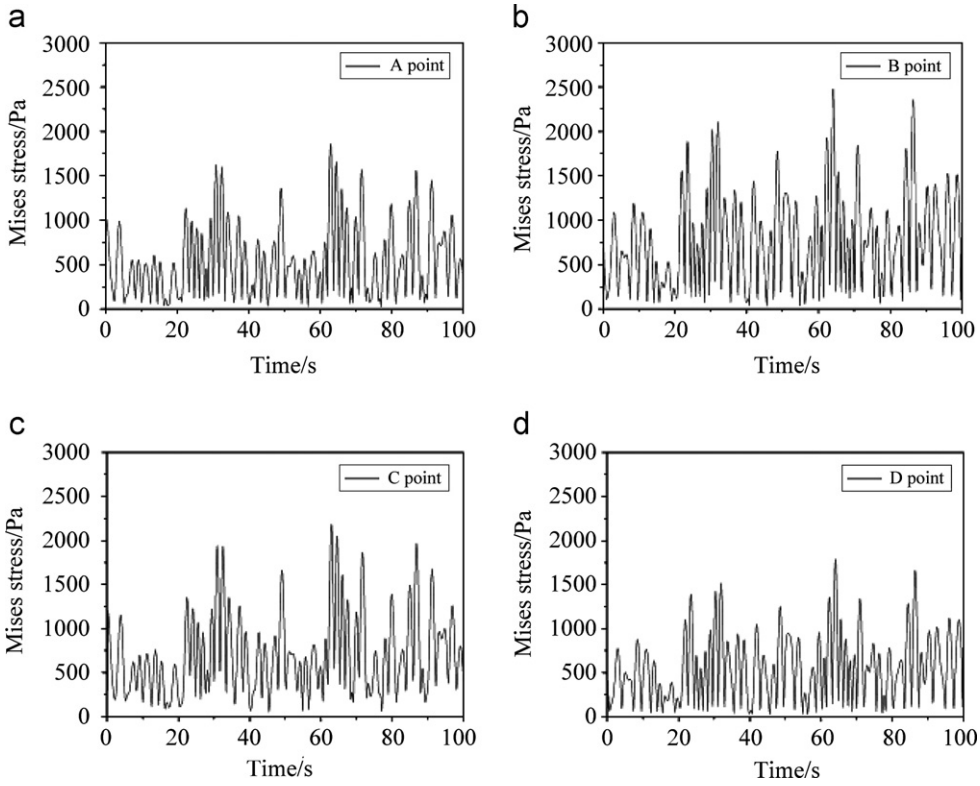

Figure 12 Mises stress vs. time of critical areas. (a) Mises stress of A, (b) Mises stress of B, (c) Mises stress of C and (d) Mises stress of D.

(2) The maximum Mises stress amplitude is in critical area B, so the cumulative damage of this area should be researched in the future.

References

[1] K. Zhou, Z.X. Zhu, Y. Yang, Simulation of ocean wave in the northwest Pacific Ocean, Journal of Zhejiang University (Science Edition) 36 (5) (2009) 603–608 (in Chinese).

[2] B. Wen, Y.L. Zhao, Z.J. Chen, J.P. Wang, Numerical computation and statistic analysis on the ocean wave field in north Indian Ocean, Marine Science Bulletin 29 (5) (2010) 493–498 (in Chinese).

[3] Y.G. Xing, G.W. Jin, X.C. Xu, B.X. Hou, H.F. Liu, K.H. Dong, Comprehensive property tests and service life evaluation for solid rocket motors, Journal of Propulsion Technology 25 (2) (2004) 176–179 (in Chinese).

[4] J.Z. Xu, D.M. Jia, Research of analysismethod for storage life of SRM, Journal of Solid Rocket Technology 32 (3) (2009) 271–273 (in Chinese).

[5] Y.G. Xing, K. Qu, J.S. Xu, G.C. Li, Life prediction of solid rocket motor under the ship swing motion, Journal of Propulsion Technology 32 (1) (2011) 32–36 (in Chinese).

[6] K. Qu, Y.G. Xing, X.D. Zhang, Fatigue damage of shipborne solid rocket motor propellant under swing loading, Journal of Aerospace Power 26 (11) (2011) 2636–2640 (in Chinese).

[7] J.S. Xu, Life prediction of solid motor grain under the influence of ship swing load based on the dissipated energy method, Ph.M. Dissertation, Naval Aeronautical Engineering Institute, Yantai, Shandong, 2009 (in Chinese).

[8] S.M. Vanden Berg, Non-linear rolling of ships in large sea waves, Ph.M. Dissertation, Naval Postgraduate School, Monterey, California, 2007.